World Journal of Gastroenterology

Submit a Manuscript: http://www.f6publishing.com

World J Gastroenterol 2017 May 14; 23(18): 3279-3286

DOI: 10.3748/wjg.v23.i18.3279

ISSN 1007-9327 (print) ISSN 2219-2840 (online)

ORIGINAL ARTICLE

Basic Study

Wall shear stress in portal vein of cirrhotic patients with portal hypertension

Wei Wei, Yan-Song Pu, Xin-Kai Wang, An Jiang, Rui Zhou, Yu Li, Qiu-Juan Zhang, Ya-Juan Wei, Bin Chen, Zong-Fang Li

Wei Wei, Yu Li, Zong-Fang Li, National and Local Joint Engineering Research Center of Biodiagnosis and Biotherapy, the Second Affiliated Hospital of Xi'an Jiaotong University, Xi'an 710004, Shaanxi Province, China

Yan-Song Pu, An Jiang, Rui Zhou, Qiu-Juan Zhang, Ya-Juan Wei, Shaanxi Provincial Clinical Research Center for Hepatic and Splenic Diseases, The Second Affiliated Hospital of Xi'an Jiaotong University, Xi'an 710004, Shaanxi Province, China

Xin-Kai Wang, Bin Chen, State Key Laboratory of Multiphase Flow in Power Engineering, Xi'an Jiaotong University, Xi'an 710049, Shaanxi Province, China

Author contributions: Wei W and Pu YS contributed equally to this work; Wei W, Pu YS and Li ZF designed the research; Jiang A, Zhou R, Li Y, Zhang QJ and Wei YJ collected the clinical data; Wang XK and Chen B contributed to the computational fluid dynamics remodeling; Wei W and Pu YS analyzed the data; Wei W and Li ZF wrote the paper.

Supported by the Program for Changjiang Scholars and Innovative Research Team in Universities, No. PCSIRT-1171; National Natural Science Foundation of China, No. 81270504; Fundamental Research Funds for the Central Universities, No. xjj20100209.

Institutional review board statement: This study was reviewed and approved by the Institutional Review Board of The Second Affiliated Hospital of Xi'an Jiaotong University.

Conflict-of-interest statement: All authors declare no conflicts of interest related to this study.

Data sharing statement: No additional data are available.

Manuscript source: Invited manuscript

Correspondence to: Zong-Fang Li, MD, PhD, Professor, National and Local Joint Engineering Research Center of Biodiagnosis and Biotherapy, The Second Affiliated Hospital of Xi'an Jiaotong University, No. 157 Xiwu Road, Xi'an 710004, Shaanxi Province, China. lzf2568@gmail.com
Telephone: +86-29-87679508
Fax: +86-29-87678634

Received: December 28, 2016
Peer-review started: December 30, 2016
First decision: January 19, 2017
Revised: February 3, 2017
Accepted: March 3, 2017
Article in press: March 3, 2017
Published online: May 14, 2017

Abstract

AIM

To investigate wall shear stress (WSS) magnitude and distribution in cirrhotic patients with portal hypertension using computational fluid dynamics.

METHODS

Idealized portal vein (PV) system models were reconstructed with different angles of the PV-splenic vein (SV) and superior mesenteric vein (SMV)-SV. Patient-specific models were created according to enhanced computed tomography images. WSS was simulated by using a finite-element analyzer, regarding the blood as a Newtonian fluid and the vessel as a rigid wall. Analysis was carried out to compare the WSS

in the portal hypertension group with that in healthy controls.

RESULTS

For the idealized models, WSS in the portal hypertension group (0-10 dyn/cm^2) was significantly lower than that in the healthy controls (10-20 dyn/cm^2), and low WSS area (0-1 dyn/cm^2) only occurred in the left wall of the PV in the portal hypertension group. Different angles of PV-SV and SMV-SV had different effects on the magnitude and distribution of WSS, and low WSS area often occurred in smaller PV-SV angle and larger SMV-SV angle. In the patient-specific models, WSS in the cirrhotic patients with portal hypertension (10.13 ± 1.34 dyn/cm^2) was also significantly lower than that in the healthy controls (P < 0.05). Low WSS area often occurred in the junction area of SV and SMV into the PV, in the area of the division of PV into left and right PV, and in the outer wall of the curving SV in the control group. In the cirrhotic patients with portal hypertension, the low WSS area extended to wider levels and the magnitude of WSS reached lower levels, thereby being more prone to disturbed flow occurrence.

CONCLUSION

Cirrhotic patients with portal hypertension show dramatic hemodynamic changes with lower WSS and greater potential for disturbed flow, representing a possible causative factor of PV thrombosis.

Key words: Portal hypertension; Wall shear stress; Portal vein system; Distribution; Disturbed flow

Core tip: For portal hypertension, idealized portal vein (PV) modeling showed a significantly lower wall shear stress (WSS) in both sides of the PV and the occurrence of disturbed flow in the left wall of the PV. In addition, greater risk of disturbed flow was found for smaller PV-splenic vein (SV) angle and larger superior mesenteric vein-SV angle. In patient-specific models, WSS in cirrhotic patients with portal hypertension was markedly lower than that in healthy controls and disturbed flow was more likely to occur in the portal hypertension patients.

Wei W, Pu YS, Wang XK, Jiang A, Zhou R, Li Y, Zhang QJ, Wei YJ, Chen B, Li ZF. Wall shear stress in portal vein of cirrhotic patients with portal hypertension. *World J Gastroenterol* 2017; 23(18): 3279-3286 Available from: URL: http://www.wjgnet.com/1007-9327/full/v23/i18/3279.htm DOI: http://dx.doi.org/10.3748/wjg.v23.i18.3279

INTRODUCTION

The morbidity and mortality of liver cirrhosis have been increasing in developed countries, with this disease currently representing one of the most common causes of death in adults worldwide[1]. A severe complication of liver cirrhosis is portal hypertension, which can lead to gastroesophageal varices, ascites and hepatic encephalopathy. Indeed, portal hypertension has emerged as the leading cause of mortality and liver transplantation in cirrhotic patients[2].

Pathological progress from chronic liver disease to cirrhosis is accompanied by architectural and structural changes in the hepatic microvascular system, including sinusoidal remodeling, intrahepatic shunt formation and hepatic endothelial dysfunction. As a result, intrahepatic resistance is increased; itself the initial and primary factor underlying increase in portal pressure that is characteristically observed in patients with cirrhosis. Unfortunately, the sequential adaptive response of splanchnic vasodilation (to increase liver blood supply) can serve to aggravate portal vein (PV) pressure. In patients with advanced cirrhosis, an intensively high portal hypertension (characterized by hyperdynamic splanchnic and systemic circulation) can lead to formation of portal-systemic collaterals and other complications[3]. The mean PV blood flow velocity is lower in cirrhotic patients than in healthy subjects, and Zironi *et al*[4] found that the mean velocity dropped from 19.6 ± 2.6 cm/s in normal subjects to 13.0 ± 3.2 cm/s in patients with cirrhosis. Finally, it is intriguing that abnormal PV hemodynamic changes are also closely related to PV thrombosis, a complication of advanced liver disease, but the mechanism remains to be elucidated[5,6].

Recently, the study of abnormal hemodynamic changes in atherosclerosis has gained considerable attention, with its occurrence being purported as a plausible explanation for atherosclerotic plaque formation[7]. This theory is based on the observation that the location of abnormal flow rate fits well with presence of vascular inflammation and distribution of the atherosclerotic plaques. In general, blood flow mainly shows its effect on vessels, especially on the endothelial cells that make them up, by wall shear stress (WSS), which may involve a multitude of physical and molecular mechanisms[8-10].

Abnormal hemodynamic changes have been observed in cirrhotic patients. However, whether these hemodynamic changes, especially those related to WSS, have effects on PV thrombosis in cirrhotic patients with portal hypertension remains unclear. The present study was, therefore, designed to illustrate the magnitude and distribution of WSS in PV in cirrhotic patients with portal hypertension.

Computational fluid dynamics (CFD) is a specialist area of mathematics and a branch of fluid mechanics that has been increasingly applied to cardiovascular research areas. Its greatest benefit has been to facilitate investigations into pressure and flow fields, in temporal and spatial manners, that had been previously unachievable by the traditional methods of measurement[11]. Botar *et al*[12] used the Reynolds

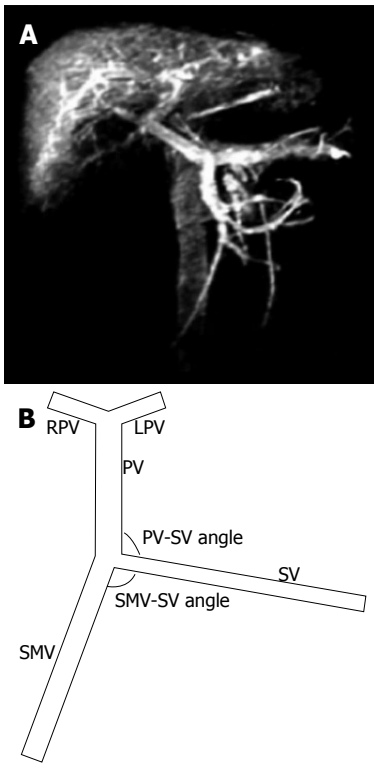

Figure 1 Geometry of the portal vein system. A: Enhanced CT of the portal vein (PV) system; B: Geometry of the idealized PV model. SV: Splenic vein; SMV: Superior mesenteric vein; LPV: Left PV; RPV: Right PV.

Table 1 Geometric and hemodynamic parameters of the idealized portal vein system model

Vein	Length (cm)	Diameter (cm)		Inlet velocity (cm/s)	
		Control	PH	Control	PH
PV	5.1	1.03	1.31	-	-
SV	9.6	0.63	0.95	17	16
SMV	8.2	0.92	0.94	21	17
LPV	2.1	0.73	0.75	-	-
RPV	2.1	0.83	0.78	-	-

PV: Portal vein; SV: Splenic vein; SMV: Superior mesenteric vein; LPV: Left PV; RPV: Right PV.

stress equation model to simulate hemodynamics in the PV system. We previously applied the CFD approach to reconstruct both idealized and patient-specific models, thereby illustrating that liver right-lobe atrophy and left-lobe hypertrophy is significantly influenced by the different distribution of blood from splenic vein (SV) and superior mesenteric vein (SMV) in patients with portal hypertension as compared to healthy control subjects[13]. When interpreting our findings from that previous CFD study and determining how to best build upon them, we considered the study by Van Steenkiste *et al*[14], in which vascular corrosion casting was used to analyze WSS in the PV of rodents with portal hypertension and cirrhosis.

In the present study, we constructed an idealized PV model and patient-specific models; the latter of which based on enhanced computed tomography (CT) images from 10 cirrhotic patients with portal hypertension and five healthy control subjects. We analyzed the WSS distribution in these models by using CFD.

MATERIALS AND METHODS

Idealized PV modeling

The PV system consists of the SV and SMV, which join to form the PV itself. The PV then goes into the liver, where it branches into the left PV (LPV) and right PV (RPV). First, we constructed an idealized but physically representative model of the PV system (Figure 1). The vessel geometric parameters (Table 1) were determined according to clinical data and literature[15], which showed that the angle between the SV and SMV ranges from 85° to 135°, while the angle between the SV and PV ranges from 90° to 130°.

We constructed and meshed the idealized models using GAMBIT 2.4.0 software. The resultant models were imported into Fluent 6.3 CFD software (Ansys), which was used to calculate the blood flow field. The WSS visualization was achieved with Tecplot 360 software.

The idealized models were divided into a control group and a portal hypertension group. The diameters of the different vessels and the velocities of the inlet vessels for those two groups are listed in Table 1. We first compared the magnitude and distribution of WSS in the control group idealized model with those in the portal hypertension group idealized model. Then, we examined a variety of SMV-SV angles (85°, 95° and 105°) and PV-SV angles (90°, 110° and 130°) to study their respective effects on WSS (Figure 1B).

Patient-specific modeling

Imaging data from all subjects were collected from enhanced CT images obtained by the GE LightSpeed 16-slice CT scanner (GE Healthcare, United States) in The Second Affiliated Hospital of Xi'an Jiaotong University between March and October 2016. The clinical characteristics of the patients diagnosed with liver cirrhosis[1] (liver biopsy confirmed) and portal hypertension and of the healthy controls (no history of liver disease) are presented in Table 2. All patients had hypersplenism and history of gastrointestinal bleeding, and many of the patients had undergone splenectomy and esophagogastric devascularization. This research was approved by the Ethical Committee of The Second Affiliated Hospital of Xi'an Jiaotong University and all enrolled subjects provided written informed consent for study participation and publication of related data.

All CT scans were performed in a supine position, and the scanning area encompassed the SMV to the bifurcation of the first porta hepatis. For each subject, each scan produced 320 layers of images with a thickness of 0.5 mm. We selected the PV phase CT images to construct the 3D models.

The geometry of the patient-specific PV models was constructed by using Mimics software for CFD

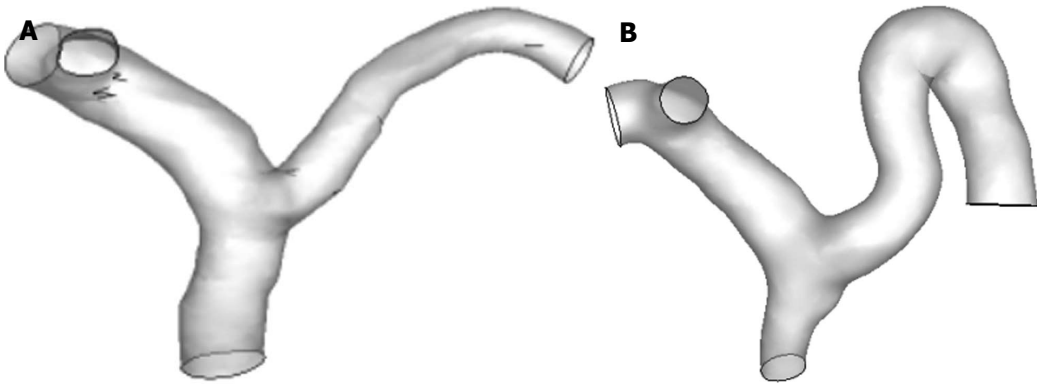

Figure 2 Geometry of the patient-specific portal vein model. A: Healthy control; B: Cirrhotic patient with portal hypertension.

Table 2 Clinical characteristics of patients with cirrhosis and portal hypertension and healthy controls

Parameters	Cirrhotic (n = 10)	Non-cirrhotic (n = 5)	P value
Sex, M/F	7/3	3/2	0.73
Age, yr	41 (31-58)	40 (29-53)	0.85
AST, in UI/L	52 (44-61)	30 (25-35)	0.01
ALT, UI/L	44 (41-56)	30 (28-31)	0.01
Platelet count, $\times 10^9$/L	48 (42-57)	235 (206-265)	< 0.01
Diameter, in mm			
PV	12.9 (11.0-14.3)	10.3 (9.9-10.7)	0.02
SV	10.0 (8.4-10.2)	6.3 (6.1-6.5)	< 0.01
SMV	8.6 (7.7-10.7)	9.3 (8.9-9.6)	0.77

Data are shown as median (interquartile range), except for age shown as median (range). ALT: Alanine transaminase; AST: Aspartate transaminase.

analysis (Materialise, Belgium), as shown in Figure 2. To facilitate the hemodynamic calculation, some small parts were pruned during the 3D reconstruction, so that only the PV and its main branches (SV, SMV, LPV and RPV) were retained. Gambit 2.4.0 software was used to remesh the geometric models; after which, the models were imported into Fluent 6.3 software to calculate the blood flow.

Numerical simulation

CFD simulations were performed by using finite-element analysis under the governing equations of mass and momentum conservation. Because the PV starts far from the heart, the influence of the cardiac cycle is negligible and can be ignored. For simplicity, the blood in the PV system demonstrated laminar flow and was assumed to be an incompressible isothermal Newtonian fluid, with a gravity of 1050 kg/m^3 and a viscosity of 4.5 × 10^{-3} N/m^2/s. The vessel wall was regarded as rigid, without slip conditions or viscoelastic properties. The boundary conditions used in all models were a constant inlet velocity for the SV and SMV.

For the idealized PV model, the average axial velocities of blood flow in the SMV and SV are listed in Table 1 for the portal hypertension and control groups. For the patient-specific PV model, the average axial velocities of blood flow in the SMV and SV of the cirrhotic patients with portal hypertension and the healthy controls were determined according to individuals' results of testing by Doppler ultrasound. A traction-free boundary condition was applied to the outlets. The outflow was weighted according to the values reported in the literature: 0.6 for the RPV and 0.4 for the LPV. WSS distributions were calculated from the velocity field data.

Data analysis

Data are represented as median or interquartile range, except for age (median and range). The WSS in patient-specific models are presented as mean ± SD. The magnitude and distribution of WSS were recorded in all idealized models and patient-specific models. The WSS between cirrhotic patients and normal subjects in the patient-specific model was compared using the Mann-Whitney U test. Analyses were carried out using SPSS version 19.0 (IBM, Chicago, IL, United States). Statistical significance was defined as two-tailed P < 0.05.

RESULTS

Differential distribution of WSS in idealized PV models of portal hypertension and control groups

To calculate the magnitude and distribution of WSS in the portal hypertension and control groups, we first constructed idealized PV models (Figure 1) according to geometric parameters, and then imported inlet velocities (Table 1) into Fluent 6.3.0. Figure 3 shows that WSS in the PV right wall was higher than that in the left wall, in both the portal hypertension and control groups. In the PV right wall, WSS was significantly decreased in the portal hypertension group (5-20 dyn/cm^2) as compared to the control group (15-30 dyn/cm^2). In the PV left wall, WSS dropped from 5-15 dyn/cm^2 in the control group to 0-5 dyn/cm^2 in the portal hypertension group, and WSS dropped to 0, demonstrating the possibility of disturbed flow. Table 3 lists the mean WSS in left and right walls of the PV in the portal hypertension and control groups.

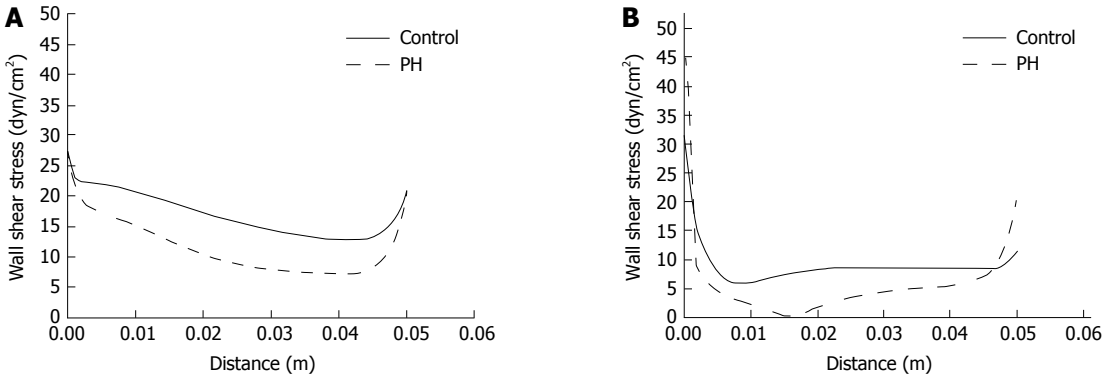

Figure 3 Wall shear stress distribution in right wall (A) and left wall (B) in the healthy control and portal hypertension groups. The X axis shows the length of the side wall of the PV, starting from 0 in the junction of SV and SMV. The Y axis shows WSS. SV: Splenic vein; SMV: Superior mesenteric vein.

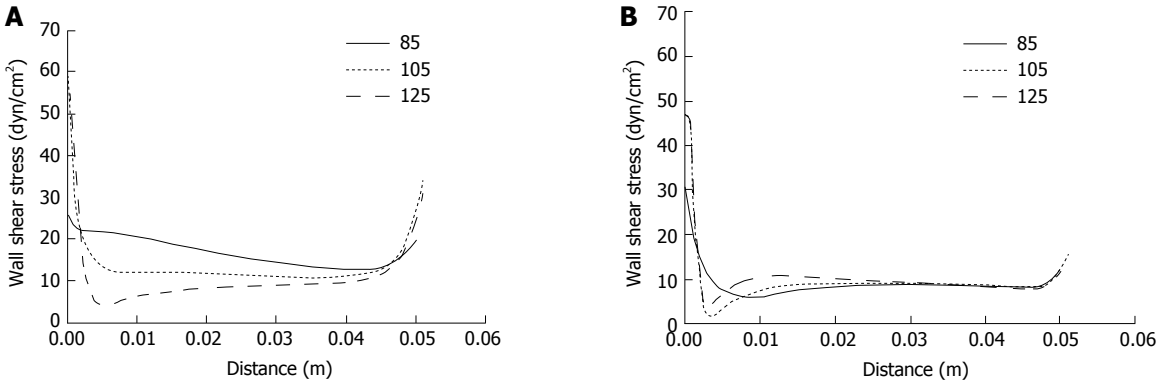

Figure 4 Wall shear stress distribution in right wall (A) and left wall (B) for different superior mesenteric vein-splenic vein angles. The X axis shows the length of the side wall of PV, starting from 0 in the junction of SV and SMV. The Y axis shows WSS. SV: Splenic vein; SMV: Superior mesenteric vein.

Table 3 Wall shear stress in left and right walls of the portal vein in control and portal hypertension groups

	Control group		PH group	
	Right wall	Left wall	Right wall	Left wall
WSS, dyn/cm^2	16.3	8.6	9.8	4.4

Data are shown as median. PH: Portal hypertension. WSS: Wall shear stress.

Table 4 Wall shear stress in right and left walls for different superior mesenteric vein-splenic vein angles

	Right wall			Left wall		
	85°	105°	125°	85°	105°	125°
WSS, dyn/cm^2	16.3	12.1	9	8.6	8.7	9.4

Data are shown as median. WSS: Wall shear stress.

Differential effects of SMV-SV and PV-SV angles on WSS distribution in idealized PV models

Due to the complicity and variation of the PV system that exists among individuals in real life, we investigated the effects of different SMV-SV and PV-SV angles on WSS distribution in the PV. According to the ranges of real-life angles for PV-SV and SMV-SV, we selected 90°, 110° and 130° to examine the former and 85°, 105° and 125° to examine the latter by idealized models. As shown in Figure 4, the effects of SMV-SV angle variation mainly involved the proximal portion of the PV. The magnitude of WSS was found to decrease as the angle increased in the PV right wall, but no similar change was found in the PV left wall. WSS distribution in the proximal left wall changed when the angle increased, supporting the possibility of disturbed flow occurrence. In the right wall, a greater possibility of disturbed flow followed with the angle > 125°. Table 4 shows the mean WSS in the right wall and left wall of the PV for the different SMV-SV angles.

The effects of PV-SV angle variation also mainly involved the proximal portion of the PV (Figure 5). As the angle increased, the magnitude of WSS decreased in the right wall but increased in the left wall. Moreover, disturbed flow occurred with PV-SV angle of 90°, disappearing with any increase in the angle. Table 5 shows the mean WSS in the right wall and left wall of the PV for the different PV-SV angles.

Patient-specific models

To simulate the WSS in real-life PV systems, we reconstructed patient-specific models from 10 patients with cirrhotic portal hypertension and five healthy subjects who served as controls. The clinical data for

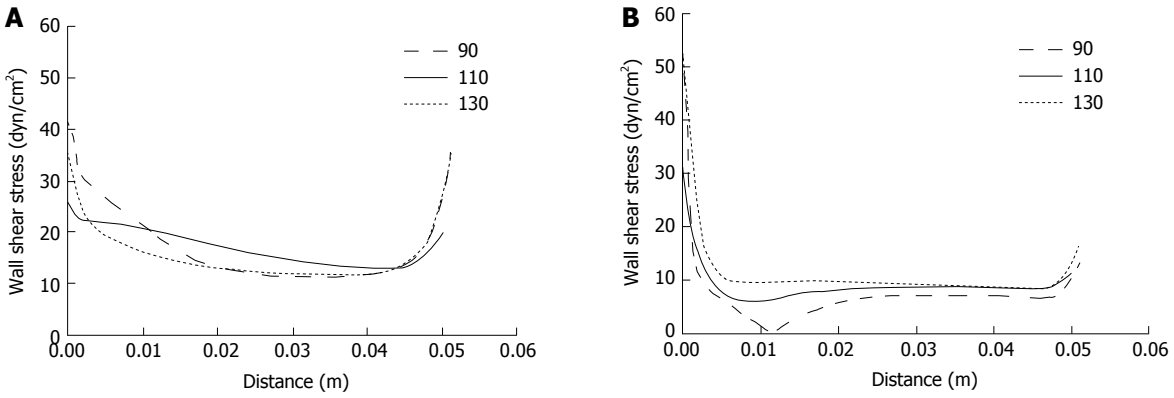

Figure 5 Wall shear stress distribution in right wall (A) and left wall (B) for different portal vein-splenic vein angles. The X axis shows the length of the side wall of PV, starting from 0 in the junction of SV and SMV. The Y axis shows WSS. SV: Splenic vein; SMV: Superior mesenteric vein.

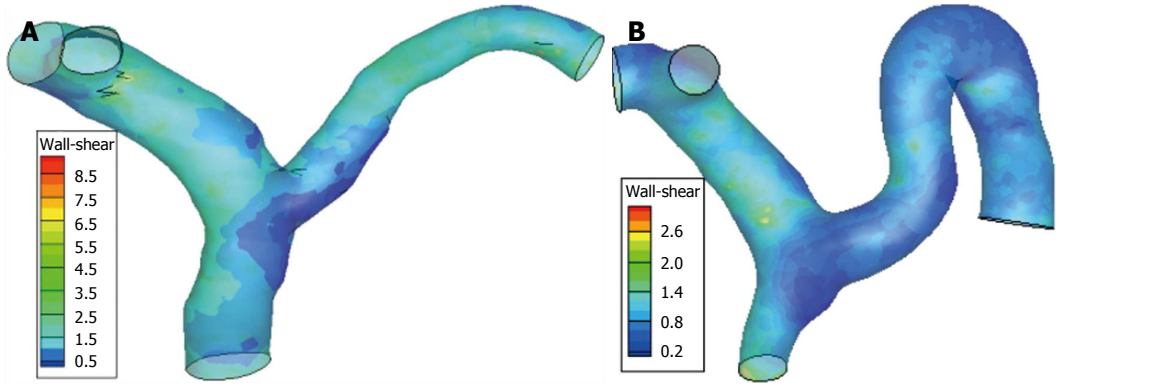

Figure 6 Portal vein system wall shear stress distribution in healthy controls (A) and cirrhotic patients with portal hypertension (B).

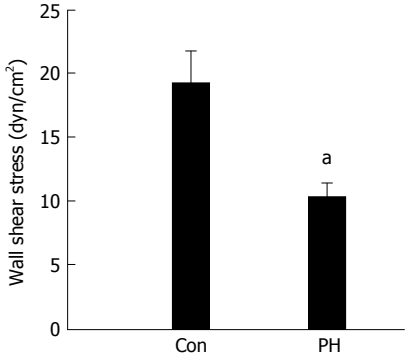

Figure 7 Mean wall shear stress of portal vein in healthy controls (Con) and cirrhotic patients with portal hypertension. [a]*P* < 0.05 *vs* healthy controls.

each group is shown in Table 2, which includes the finding that the SV and PV diameters in the patients were significantly larger than those in the controls, and that the SMV diameter did not differ between patients and healthy subjects.

Figures 6 and 7 show the WSS distributions in the PV systems of the patients and controls. The mean WSS in the patients (10.13 ± 1.34 dyn/cm^2) was significantly higher than that in the controls (19.06 ± 2.63 dyn/cm^2), and these results agree well with those from the idealized model simulations ($P < 0.05$). Disturbed flow occurred more readily in low shear stress areas. In the controls, low shear stress areas were found in the junctional area of SV and SMV into the PV, the divided area of the PV into LPV and RPV, and the outer wall of curving SV. In the patients, low shear stress areas extended wider and the magnitude of WSS was lower, signifying a greater propensity towards occurrence of disturbed flow.

Table 5 Wall shear stress in left and right walls for different portal vein-splenic vein angles

	Right wall			Left wall		
	90°	110°	130°	90°	110°	130°
WSS, dyn/cm^2	13.7	16.3	13.3	6.9	8.6	9.7

Data are shown as median. WSS: Wall shear stress.

DISCUSSION

Hemodynamic changes, especially WSS, create adverse effects in cardiovascular disease. As a preliminary study to illuminate whether biomechanical forces have effects on hepatic PV diseases, such as PV thrombosis, we reconstructed idealized PV models and patient-specific models and quantified the magnitude and distribution of WSS in portal hypertension patients for comparison with those of healthy controls.

We found that the magnitude of WSS in the portal hypertension group was significantly lower than that in the healthy control group (both for idealized and the patient-specific modeling).

The magnitude and distribution of WSS have been investigated in the cardiovascular system. These studies generally use Poiseuille's law to determine the magnitude of WSS[16]. According to literature, the WSS ranges from 1 to 6 dyn/cm^2 in the venous system and from 10 to 79 dyn/cm^2 in the arterial system[17]. Among the CFD-based research studies of the cardiovascular system, Soulis *et al*[18] reported simulating the WSS in the normal left coronary tree; their results indicated high WSS regions occurring often at all flow dividers and low WSS regions (7.5-22.5 dyn/cm^2) occurring at bifurcations opposite the flow dividers. Shojima *et al*[19] reported findings that WSS in the vessel region of a middle cerebral artery aneurysm was significantly lower than that in the neck region (36.4 ± 12.5 *vs* 143.9 ± 62.1 dyn/cm^2) and markedly higher than that in the aneurysm region (16.4 ± 11.6 dyn/cm^2). Tang *et al*[20] showed that WSS in pulmonary arterial hypertension patients is significantly lower than in controls (4.3 ± 2.8 *vs* 20.5 ± 4.0 dyn/cm^2) for the central pulmonary artery, unlike the distal artery which showed no difference.

In the current study, we found that WSS in cirrhotic patients was significantly lower than in healthy controls. Low WSS area, which carries a greater possibility of disturbed flow, was found to most often occur with larger PV-SMV angle and smaller PV-SV angle. We also found that the low WSS area often occurred in the junction area of SV and SMV into PV, the divided area of PV into LPV and RPV, and the outer wall of curving SV for the healthy controls, and that this area extended wider and had lower magnitude in the cirrhotic patients with portal hypertension.

Endothelial cells are constantly exposed to WSS, which is known to be able to trigger and regulate various endothelial cell functions. Clinical studies have found that atherosclerotic plaques preferentially develop at regions with disturbed flow and low WSS, such as branches, bifurcations and curvatures[21-23]. Under conditions of oscillatory and low WSS, endothelial cells have been shown to have a proinflammatory phenotype, with increased procoagulant and proadhesive properties and decreased production of nitric oxide[24].

In the development of portal hypertension, endothelial dysfunction plays fundamental roles in initiating intrahepatic vascular resistance; moreover, liver sinusoidal endothelial cells attain a hypoactive phenotype that is characterized by decreased production of nitric oxide[25]. Furthermore, PV thrombosis reportedly has higher prevalence (0.6%-15.8%) in cirrhotic patients with portal hypertension, and reduced portal flow velocity has been proposed as the most important predictive parameter of this condition[5]. To date, however, there is no such research about the effects of abnormal PV system WSS on endothelial dysfunction, nor on whether the dysfunctional endothelial cells play important roles in PV diseases, such as PV thrombosis. Our simulation data fill this gap in the field and may serve as a basis for future *in vitro* studies.

However, several limitations inherent to the study design must be considered when extrapolating our findings. First, our real-life study population included a small number of cirrhotic patients with portal hypertension. Moreover, we enrolled only patients waiting for splenectomy; as such, our results cannot be generalized to patients with mild to moderate portal hypertension. In addition, other portal hypertension patients were excluded. Second, the correlation between low WSS areas and PV thrombosis locations has not yet been clarified.

Despite these limitations, several conclusions can be drawn based upon careful consideration of the available data. Cirrhotic patients with portal hypertension present noticeable hemodynamic changes, which were indicated by lower WSS and a greater likelihood of disturbed flow. Future investigations on this topic should be designed with a stratification approach, to further differentiate portal hypertension patients, for example, according to severity of their disease in order to determine the specificity and sensitivity of WSS and its clinical applicability.

COMMENTS

Background

Hemodynamic changes, especially wall shear stress (WSS), create adverse effects on endothelial function in cardiovascular disease. Endothelial dysfunction and abnormal hemodynamic changes are known to play important roles in portal hypertension, which may lead to portal vein (PV)-associated diseases, such as PV thrombosis. However, there is sparse research on the distribution of WSS in the PV system in portal hypertension, the effects of abnormal PV system WSS on endothelial dysfunction, and whether the dysfunctional endothelial cells play important roles in PV diseases.

Research frontiers

This study demonstrated that WSS was significantly lower in both sides of the PV for the portal hypertension group as compared with the normal controls, shown by idealized PV modeling. Moreover, disturbed flow was more prone to occur in the left wall of the PV in the portal hypertension group. In addition, greater risk of disturbed flow was found for smaller PV-splenic vein (SV) angle and larger superior mesenteric vein-SV angle. In patient-specific models, WSS in cirrhotic patients with portal hypertension was markedly lower than that in healthy controls and disturbed flow was more likely to occur in the portal hypertension patients.

Innovations and breakthroughs

This research simulated the magnitude and distribution of WSS using both idealized PV models and patient-specific models and found that WSS was significantly lower in cirrhotic portal hypertension patients than in healthy controls and disturbed flow was more prone to occur in portal hypertension patients.

Applications

This simulation data can fill the current gap in the field of WSS distribution in cirrhotic portal hypertension patients and may serve as a basis for future *in vitro* studies to explore the effects of abnormal WSS in portal hypertension on endothelial dysfunction and PV diseases, such as PV thrombosis.

Terminology

WSS is generated by blood flow viscosity acting upon the luminal vessel wall and exerts a frictional force per unit on endothelial surface of vessels. Computational fluid dynamics is a specialist area of mathematics and a branch of fluid mechanics; its greatest benefit has been to facilitate investigations into pressure and flow fields, in temporal and spatial manners that had been previously unachievable by the traditional methods of measurement.

Peer-review

This is a study regarding WSS simulation in cirrhotic portal hypertension patients using computational fluid dynamics. Generally, the simulation was performed properly and the manuscript was well-written. The main findings are quite novel and can provide basic data to simulate portal hypertension WSS for future *in vitro* studies.

REFERENCES

1 **Tsochatzis EA**, Bosch J, Burroughs AK. Liver cirrhosis. *Lancet* 2014; **383**: 1749-1761 [PMID: 24480518 DOI: 10.1016/s0140-6736(14)60121-5]

2 **de Franchis R**. Expanding consensus in portal hypertension: Report of the Baveno VI Consensus Workshop: Stratifying risk and individualizing care for portal hypertension. *J Hepatol* 2015; **63**: 743-752 [PMID: 26047908 DOI: 10.1016/j.jhep.2015.05.022]

3 **García-Pagán JC**, Gracia-Sancho J, Bosch J. Functional aspects on the pathophysiology of portal hypertension in cirrhosis. *J Hepatol* 2012; **57**: 458-461 [PMID: 22504334 DOI: 10.1016/j.jhep.2012.03.007]

4 **Zironi G**, Gaiani S, Fenyves D, Rigamonti A, Bolondi L, Barbara L. Value of measurement of mean portal flow velocity by Doppler flowmetry in the diagnosis of portal hypertension. *J Hepatol* 1992; **16**: 298-303 [PMID: 1487606 DOI: 10.1016/s0168-8278(05)80660-9]

5 **Kinjo N**, Kawanaka H, Akahoshi T, Matsumoto Y, Kamori M, Nagao Y, Hashimoto N, Uehara H, Tomikawa M, Shirabe K, Maehara Y. Portal vein thrombosis in liver cirrhosis. *World J Hepatol* 2014; **6**: 64-71 [PMID: 24575165 DOI: 10.4254/wjh.v6.i2.64]

6 **Zhang Y**, Wen TF, Yan LN, Yang HJ, Deng XF, Li C, Wang C, Liang GL. Preoperative predictors of portal vein thrombosis after splenectomy with periesophagogastric devascularization. *World J Gastroenterol* 2012; **18**: 1834-1839 [PMID: 22553410 DOI: 10.3748/wjg.v18.i15.1834]

7 **Gimbrone MA**, García-Cardeña G. Vascular endothelium, hemodynamics, and the pathobiology of atherosclerosis. *Cardiovasc Pathol* 2013; **22**: 9-15 [PMID: 22818581 DOI: 10.1016/j.carpath.2012.06.006]

8 **Chien S**. Mechanotransduction and endothelial cell homeostasis: the wisdom of the cell. *Am J Physiol Heart Circ Physiol* 2007; **292**: H1209-H1224 [PMID: 17098825 DOI: 10.1152/ajpheart.01047.2006]

9 **Zhou J**, Li YS, Chien S. Shear stress-initiated signaling and its regulation of endothelial function. *Arterioscler Thromb Vasc Biol* 2014; **34**: 2191-2198 [PMID: 24876354 DOI: 10.1161/atvbaha.114.303422]

10 **Marin T**, Gongol B, Chen Z, Woo B, Subramaniam S, Chien S, Shyy JY. Mechanosensitive microRNAs-role in endothelial responses to shear stress and redox state. *Free Radic Biol Med* 2013; **64**: 61-68 [PMID: 23727269 DOI: 10.1016/j.freeradbiomed.2013.05.034]

11 **Morris PD**, Narracott A, von Tengg-Kobligk H, Silva Soto DA, Hsiao S, Lungu A, Evans P, Bressloff NW, Lawford PV, Hose DR, Gunn JP. Computational fluid dynamics modelling in cardiovascular medicine. *Heart* 2016; **102**: 18-28 [PMID: 26512019 DOI: 10.1136/heartjnl-2015-308044]

12 **Botar CC**, Vasile T, Sfrangeu S, Clichici S, Agachi PS, Badea R, Mircea P, Cristea MV, Moldovan R. CFD Simulation of the Portal Vein Blood Flow[C] International Conference on Advancements of Medicine and Health Care through Technology. Springer Berlin Heidelberg, 2009: 359-362 [DOI: 10.1007/978-3-642-04292-8_79]

13 **Li X**, Wang XK, Chen B, Pu YS, Li ZF, Nie P, Su K. Computational hemodynamics of portal vein hypertension in hepatic cirrhosis patients. *Biomed Mater Eng* 2015; **26** Suppl 1: S233-S243 [PMID: 26406008 DOI: 10.3233/bme-151310]

14 **Van Steenkiste C**, Trachet B, Casteleyn C, van Loo D, Van Hoorebeke L, Segers P, Geerts A, Van Vlierberghe H, Colle I. Vascular corrosion casting: analyzing wall shear stress in the portal vein and vascular abnormalities in portal hypertensive and cirrhotic rodents. *Lab Invest* 2010; **90**: 1558-1572 [PMID: 20714322 DOI: 10.1038/labinvest.2010.138]

15 **George SM**. Hemodynamic investigation of the liver using magnetic resonance imaging and computational fluid dynamics. Georgia Institute of Technology, 2008: 44-45

16 **Katritsis D**, Kaiktsis L, Chaniotis A, Pantos J, Efstathopoulos EP, Marmarelis V. Wall shear stress: theoretical considerations and methods of measurement. *Prog Cardiovasc Dis* 2007; **49**: 307-329 [PMID: 17329179 DOI: 10.1016/j.pcad.2006.11.001]

17 **Malek AM**, Alper SL, Izumo S. Hemodynamic shear stress and its role in atherosclerosis. *JAMA* 1999; **282**: 2035-2042 [PMID: 10591386 DOI: 10.1001/jama.282.21.2035]

18 **Soulis JV**, Farmakis TM, Giannoglou GD, Louridas GE. Wall shear stress in normal left coronary artery tree. *J Biomech* 2006; **39**: 742-749 [PMID: 16439244 DOI: 10.1016/j.jbiomech.2004.12.026]

19 **Shojima M**, Oshima M, Takagi K, Torii R, Hayakawa M, Katada K, Morita A, Kirino T. Magnitude and role of wall shear stress on cerebral aneurysm: computational fluid dynamic study of 20 middle cerebral artery aneurysms. *Stroke* 2004; **35**: 2500-2505 [PMID: 15514200 DOI: 10.1161/01.STR.0000144648.89172.of]

20 **Tang BT**, Pickard SS, Chan FP, Tsao PS, Taylor CA, Feinstein JA. Wall shear stress is decreased in the pulmonary arteries of patients with pulmonary arterial hypertension: An image-based, computational fluid dynamics study. *Pulm Circ* 2012; **2**: 470-476 [PMID: 23372931 DOI: 10.4103/2045-8932.105035]

21 **Peiffer V**, Sherwin SJ, Weinberg PD. Does low and oscillatory wall shear stress correlate spatially with early atherosclerosis? A systematic review. *Cardiovasc Res* 2013; **99**: 242-250 [PMID: 23459102 DOI: 10.1093/cvr/cvt044]

22 **Phinikaridou A**, Hua N, Pham T, Hamilton JA. Regions of low endothelial shear stress colocalize with positive vascular remodeling and atherosclerotic plaque disruption: an in vivo magnetic resonance imaging study. *Circ Cardiovasc Imaging* 2013; **6**: 302-310 [PMID: 23357244 DOI: 10.1161/circimaging.112.000176]

23 **Wentzel JJ**, Chatzizisis YS, Gijsen FJ, Giannoglou GD, Feldman CL, Stone PH. Endothelial shear stress in the evolution of coronary atherosclerotic plaque and vascular remodelling: current understanding and remaining questions. *Cardiovasc Res* 2012; **96**: 234-243 [PMID: 22752349 DOI: 10.1093/cvr/cvs217]

24 **Hsieh HJ**, Liu CA, Huang B, Tseng AH, Wang DL. Shear-induced endothelial mechanotransduction: the interplay between reactive oxygen species (ROS) and nitric oxide (NO) and the pathophysiological implications. *J Biomed Sci* 2014; **21**: 3 [PMID: 24410814 DOI: 10.1186/1423-0127-21-3]

25 **Iwakiri Y**. Endothelial dysfunction in the regulation of cirrhosis and portal hypertension. *Liver Int* 2012; **32**: 199-213 [PMID: 21745318 DOI: 10.1111/j.1478-3231.2011.02579.x]

P- Reviewer: Sandow SL **S- Editor**: Qi Y **L- Editor**: Kerr C
E- Editor: Zhang FF

Published by **Baishideng Publishing Group Inc**
7901 Stoneridge Drive, Suite 501, Pleasanton, CA 94588, USA
Telephone: +1-925-223-8242
Fax: +1-925-223-8243
E-mail: bpgoffice@wjgnet.com
Help Desk: http://www.f6publishing.com/helpdesk
http://www.wjgnet.com

ISSN 1007-9327